JOURNAL OF CATALYSIS **165,** 45–56 (1997)
ARTICLE NO. CA971463

The Nature of Ruthenium Sulfide Clusters Encaged in a Y Zeolite

Bernard Moraweck, Gérard Bergeret, Martine Cattenot, Vassilios Kougionas,[1] Christophe Geantet, Jean-Louis Portefaix, José Luiz Zotin,[2] and Michèle Breysse[3]

Institut de Recherches sur la Catalyse, CNRS, 2 avenue Albert Einstein, 69626 Villeurbanne, France

Received March 23, 1996; revised August 15, 1996; accepted September 3, 1996

Catalysts of ruthenium sulfide supported in a dealuminated KY zeolite were prepared by ion exchange and subsequent sulfidation using several atmospheres containing sulfur. They were characterized by means of HREM, EDX, TPR, and EXAFS. The activity for the tetralin hydrogenation, carried out in presence of large amounts of H_2S (1.85%), was very high and roughly 300 times the activity (expressed per metal atom) of an industrial $NiMo/Al_2O_3$ hydrotreating catalyst. A simple modeling of the results obtained by the physicochemical techniques suggests that the active phase consists of clusters of less than 50 ruthenium atoms of a ruthenium sulfide-like phase with very small domains of ruthenium metal.

INTRODUCTION

At present, much research focuses on improving hydrotreating catalysts. It is particularly important to examine the hydrogenation properties of these catalysts, because hydrogenation steps are involved in the hydrodesulfurization (HDS) and hydrodenitrogenation (HDN) reaction networks. Moreover, the aromatic content of gas oils will probably be limited in the near future. The main difficulty in performing these hydrogenation reactions is the high amount of sulfur compounds present in the feeds which, after desulfurization, are converted to H_2S. Under these conditions, metallic catalysts cannot be used without a drastic decrease in the H_2S partial pressure and, therefore, two-stage processes have been designed. In order to avoid such a complexity, the design of hydrogenating catalysts, capable of maintaining their properties under a wide range of H_2S partial pressures, is of prime importance. With this objective, it seems appropriate to study ruthenium sulfide-based catalysts, because in the unsupported state, ruthenium sulfide was found to exhibit prominent hydrogenation properties (1). Furthermore, Harvey and Matheson (2) and we (3, 4) showed that ruthenium sulfide dispersed in Y zeolites is very active for the hydrogenation of nitrogen containing molecules. The interest in dispersing ruthenium in zeolite is twofold. A highly dispersed phase, more active than that on a conventional alumina support, may allow the reduction of the ruthenium content and thus the catalyst cost. Second, the zeolite framework may influence the properties of the active phase as was shown for metal catalysts. The interest in zeolites as supports for sulfide catalysts is important, and numerous recent studies have dealt with this subject (5–7). However, the characterization of these catalysts is difficult due to the high dispersion of the active phase and its location inside or outside the zeolite framework. In particular, the exact nature of the active phase is unclear. The objective of the present paper is to clarify the nature of the particles of ruthenium sulfide encaged in an ultrastable zeolite exchanged with potassium. The sulfided state of the catalysts was varied by using various sulfiding conditions. Similarly, catalytic tests for the hydrogenation of tetralin were performed in the presence of various H_2S partial pressures. The choice of the support was dictated by the possible utilization of this catalyst in a hydrotreating process. Nondealuminated Y zeolite could not be envisaged as a support for this kind of reaction due to the restricted access of the large molecules present in gas oils to the active phase when it is dispersed within the zeolite. On the other hand, we used K-exchanged zeolite in order to avoid the high acidity of the HY zeolite which could lead to severe coking and consequently to deactivation of the catalyst. The properties of the active phase were characterized by HREM and EXAFS after sulfiding in various atmospheres and after tests. The hydrogenation of tetralin was chosen as a model hydrogenation reaction of a partially saturated aromatic compound.

EXPERIMENTAL

Catalysts

Dealuminated zeolite KYd was prepared from a commercial ultrastable HYd zeolite supplied by Conteka (ref.

[1] Present address: National Technical University of Athens, Chemical Engineering Department, Section III, Materials Science and Technology, Zografou Campus, 9 Iroon Polytechniou Street, 15780 Athens, Greece.
[2] Present address: Petrobras S.A., Cenpes/Dicat—Cidade Universitaria—QD.7, Ilha do Fundão, 21949-900 Rio de Janeiro, R.J. Brazil.
[3] Fax (33) 4 72 44 53 99. E-mail: breysse@catalyse.univ-lyon1.fr.

0021-9517/97 $25.00

TABLE 1

Elemental Chemical Analysis of the Support and the Catalyst

Catalyst	Concentration (wt%)					Si/Al atomic ratio
	Si	Al	Na	K	Ru	
HYd			0.1			6.0
KYd	40.5	6.3	0.1	3.0		6.2
RuKYd	35.2	5.8		0.4	1.8	5.9

CBV 712, overall Si/Al = 6). Exchange by potassium was achieved by two successive ion exchanges in an aqueous solution of KNO_3 (1M) at 333 K. The elemental chemical analysis of the samples is given in Table 1.

In preparating zeolite KYd from the commercial ultrastable zeolite HYd, the ion exchange was incomplete. The number of K atoms that are usually exchanged is determined by the number of Al atoms in the zeolite framework. Thus, it can be calculated that the expected amount of potassium in KYd is 8.4 wt% compared to the only 3% of K actually obtained (Table 1). The low percentage of K obtained in KYd can be probably attributed to the high proportion of extra-framework aluminum species present on the starting HYd zeolite. These species should not be taken into account in the calculation of the expected amount of K in KYd. These extra-framework aluminum species are the residuals of the dealumination process which were not completely removed by acid leaching.

The presence of the extra-framework aluminum species was confirmed by the examination of HYd and KYd by NMR of ^{29}Si; this method can detect only the atoms in the framework. The NMR of ^{29}Si spectra of the zeolites HYd and KYd were identical; their examination gave an atomic ratio of Si/Al of 12 (aluminum fraction of 0.077) corresponding to 15 Al atoms per unit cell. Since the chemical analysis (Table 1) has given an atomic ratio of Si/Al of 6 (aluminum fraction of 0.148) it is concluded that the samples contain a high proportion of extra-framework aluminum species. In fact, 15 aluminum atoms per unit cell permit the effective exchange of 4.5 wt% of potassium. The degree of exchange obtained, however, was even lower; there are always some protons which are not easily accessible because the porosity is hindered by the extra-framework aluminum species.

Ruthenium was introduced into the KYd zeolite by means of ion exchange by stirring the zeolite in an aqueous solution of $[Ru(NH_3)_6]Cl_3$ (from Johnson–Matthey) at room temperature for 48 h. The catalyst was washed with water three times and then air-dried overnight at 393 K. The amount of Ru introduced into the zeolite given in Table 1 is lower than the expected value; this may be due to the restricted accessibility of some protons and potassium cations for ruthenium exchange. This catalyst will be referred to as RuKYd.

Samples of RuKYd were sulfided using gas flows of 15% of H_2S in H_2 or N_2 at atmospheric pressure. The temperature of the reactor was gradually increased at a rate of 10 K/min to 673 K, at which temperature it remained for 4 h. The catalyst was cooled down to room temperature under the same sulfiding atmosphere and then flushed with N_2 for 30 min. These samples, labelled RuKYd (H_2S/H_2) and RuKYd (H_2S/N_2), were characterized by HREM, TPR, and EXAFS and tested for the hydrogenation of tetralin, as will be described below. Since the sulfiding agent usually utilized in industry is dimethyldisulfide (DMDS), RuKYd was also sulfided using this sulfiding compound under a partial pressure corresponding to 15% of H_2S as in the other experiments. This sample is denoted as RuKYd ($DMDS/H_2$).

The amount of sulfur, determined by chemical analyses, was 2.2% for RuKYd (H_2S/N_2) and 1.5% for RuKYd (H_2S/H_2). The values of the overall sulfur to ruthenium ratio, calculated using these measurements, are 3.9 and 2.6, respectively. It should be stressed that this method does not allow one to distinguish between the sulfur linked to ruthenium and to the zeolite. This determination was not performed on RuKYd ($DMDS/H_2$) since, after sulfidation, cooling to room temperature in the presence of the sulfiding agent leads to the adsorption on the zeolite of high amounts of nondecomposed DMDS.

After ion exchange with potassium and ruthenium followed by sulfidation the obtained ^{29}Si NMR spectra were very similar to those obtained for the zeolite HYd. Thus, no additional dealumination took place during the different stages of catalyst preparation and activation.

For purposes of comparison, a sample was treated at 673 K under pure hydrogen (0.1 MPa). This sample will be referred to as RuKYd (H_2). It was verified by on-line mass spectroscopy that, under these conditions, the ruthenium hexamine complex was totally decomposed, and the metallic state was achieved.

A commercial $NiMo/Al_2O_3$ hydrotreating catalyst containing 9% Mo and 2.4% Ni on γ-Al_2O_3 was used as a reference. This catalyst was sulfided by H_2S/H_2 at 673 K for 4 h.

Characterization

1. Electron microscopy. Zeolite grains, to be studied by STEM-EDX or by TEM, were dispersed in pure ethanol; the suspension was stirred in an ultrasonic bath, and one drop was placed on a carbon-coated copper grid. Thin cuts of the powder were also made by embedding the catalysts in an epoxy resin and cutting them with an ultramicrotome equipped with a diamond knife. Ultra thin slices (10 to 50 nm) of sample grains were examined in a JEOL 100 CX instrument. They were also analyzed by EDX in a scanning electron microscope (Vacuum Generator HB 501).

2. Temperature-programmed reduction and oxidation. Temperature-programmed reduction experiments were

carried out in a dynamic microreactor which allowed the measurement of the amount of H_2S removed under hydrogen by the use of a specific UV photodetector ($h\nu$ photoionization detector equipped with a 10.21 eV UV light source). The detector was previously calibrated with a H_2S/H_2 mixture of known composition. The sample was flushed with nitrogen and then with a hydrogen flow of 40 cm^3/min at room temperature. The temperature was slowly raised at a rate of 2 K/min to 1073 K up to complete reduction of the solid.

A similar procedure was used for temperature-programmed oxidation experiments, but the gas phase composition was analyzed by means of a mass spectrometer (FISONS Instruments) equipped with a quadripole analyzer (VG analyzer) working in Faraday mode. A silica capillary tube heated at 473 K continuously bled off a small fraction of the gas phase into the spectrometer.

3. Extended X-ray absorption fine structure. EXAFS measurements were carried out on the D42 synchrotron beam line (DCI-LURE Orsay) with the storage ring operating at 1.85 GeV and a mean current of 250 mA. The experiments were performed in transmission mode at Ru K-edge ($E = 22.117$ keV) with a channel-cut Si (311) monochromator. The spectra were recorded over a 1000 eV energy range with an energy step of 3 eV. Three to six spectra were added before they were analyzed in a standard manner (8). After background removal, the atomic-like absorption coefficient was obtained by fitting a polynomial of convenient degree and was subsequently normalized using the method of Lengeler and Eisenberger (9). The k^3-weighted $\chi(k)$ function was then Fourier transformed in the range 3 to 13 $Å^{-1}$ using a Kaiser window ($\tau = 9$). The peak corresponding to the first coordination sphere was isolated and back-Fourier transformed into k space to determine the mean coordination number n, the bond length R, and the Debye–Waller-like factor $\Delta\sigma$, by a fitting procedure using the simplex method (10). A Ru foil (15 μm thick) sample was used to extract the experimental backscattering amplitude and phase-shift functions for the Ru–Ru pair. Moreover, an unsupported RuS_2 sample was prepared by precipitation at room temperature from an aqueous solution of $RuCl_3$ by pure H_2S and by further sulfidation in an H_2S flow at 673 K for 2 h (11). X-ray diffraction confirmed that the obtained solid has the expected pyrite structure and elemental analysis indicated a sulfur to metal ratio equal to 2.25.

The quality of the fits is estimated by a reliability factor defined as (12)

$$Q = \frac{\sum_i \left[k^3\left|\chi_i^c(k)\right| - k^3\left|\chi_i^e(k)\right|\right]^2}{\sum_i \left[k^3\chi_i^e(k)\right]^2}.$$

This parameter has the same meaning as the R factor used in the refinement of X-ray crystallographic structures (13).

Samples RuKYd (H_2S/H_2), RuKYd (H_2S/N_2), and RuKYd ($DMDS/H_2$) were examined after sulfidation and after tetralin hydrogenation tests under the conditions described below. They were transferred under dry nitrogen in a glove box to sealed containers without being exposed to air before X-ray absorption experiments.

4. Catalytic activity measurements. The catalysts were tested for the hydrogenation of tetralin. Experiments were carried out in a catalytic microreactor operated in the dynamic mode in the gas phase. The standard reaction conditions consisted of a hydrogen pressure of 4.42 MPa, a partial pressure of tetralin of 2.6 kPa, a partial pressure of H_2S 84.4 kPa (1.875%), and a temperature of 523 K. Nondiluted tetralin was introduced by means of a gas phase saturator. In order to examine the influence of the H_2S partial pressure during the catalytic tests, the H_2S partial pressure was varied from 0 to 1.875%.

The standard experimental conditions were chosen so as to be away from the thermodynamic equilibrium and thus avoid the dehydrogenation of tetralin to form naphthalene and to obtain a relatively low conversion (less than 10%) of tetralin to hydrogenated products. At these low conversions, high selectivities (≈90%) towards the hydrogenation products *cis* and *trans* decalins were obtained. (The ratio of *cis* to *trans* decalins at steady state, a temperature of 523 K, and 10% conversion of tetralin was found to be 0.70.) Small quantities of isomerisation products, such as methyl indans from the isomerisation of tetralin and methylcyclopentanes from the isomerisation of one or two of the rings of decalin, were observed. At higher conversion, the selectivity of tetralin hydrogenation to isomerisation but also to cracked products increased rapidly.

After a first stage of deactivation, which was more or less intense depending on the sulfiding procedure of the catalyst, all the samples deactivated very slowly and approximately at the same rate (Fig. 1). Consequently, the specific rates were all measured after 18 h on stream.

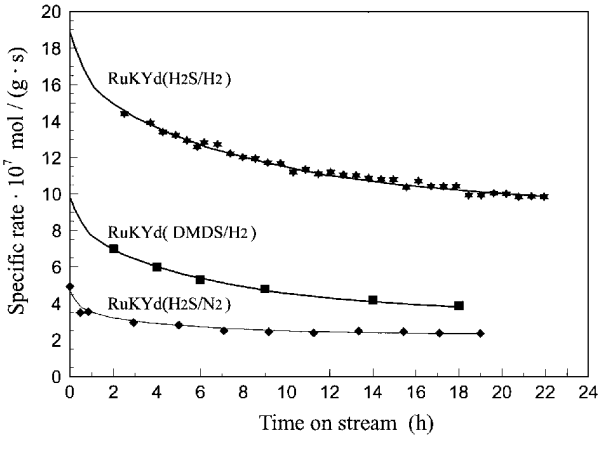

FIG. 1. Deactivation of RuKYd (H_2S/H_2), RuKYd ($DMDS/H_2$), and RuKYd (H_2S/N_2) catalysts with time on stream.

The low conversions (≤10%) used in the catalytic tests permit the application of a differential model for the determination of the specific rates of the reaction.

RESULTS

Electron Microscopy

Figures 2a through 2c show electron micrographs of RuKYd ultra-thin cuts after the sulfidation treatment. In all of these micrographs, the zeolite appears to be very well crystallized, and the pores (average diameter between 10 and 15 nm) created by the hydrothermal treatment can be observed. Ruthenium sulfide was found to consist of spherical particles homogeneously dispersed within the grains of the zeolite. The size of the particles varies with the sulfiding atmosphere. For RuKYd (H_2S/N_2) (Fig. 2a), the particle size varies from 3 to 5 nm with a few smaller particles of around 1 nm. RuKYd (DMDS/H_2) (Fig. 2b) appears to have very small particle sizes circa 1 nm and RuKYd (H_2S/H_2)

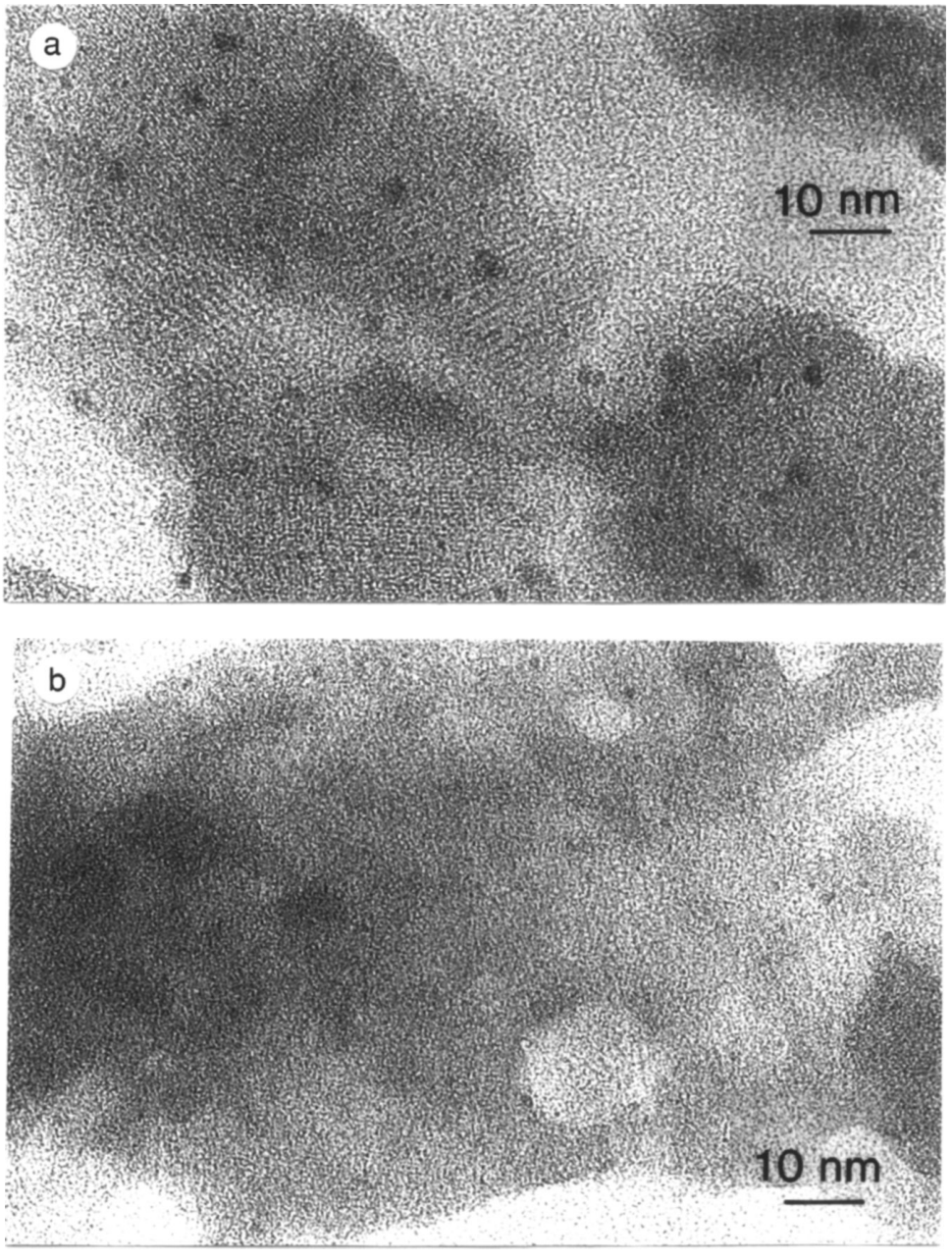

FIG. 2. Electron micrographs of RuKYd catalyst (a) sulfided by H_2S/N_2 before catalytic test, (b) sulfided by DMDS/H_2 before catalytic test, (c) sulfided by H_2S/H_2 before catalytic test, and (d) sulfided by H_2S/H_2 after catalytic test.

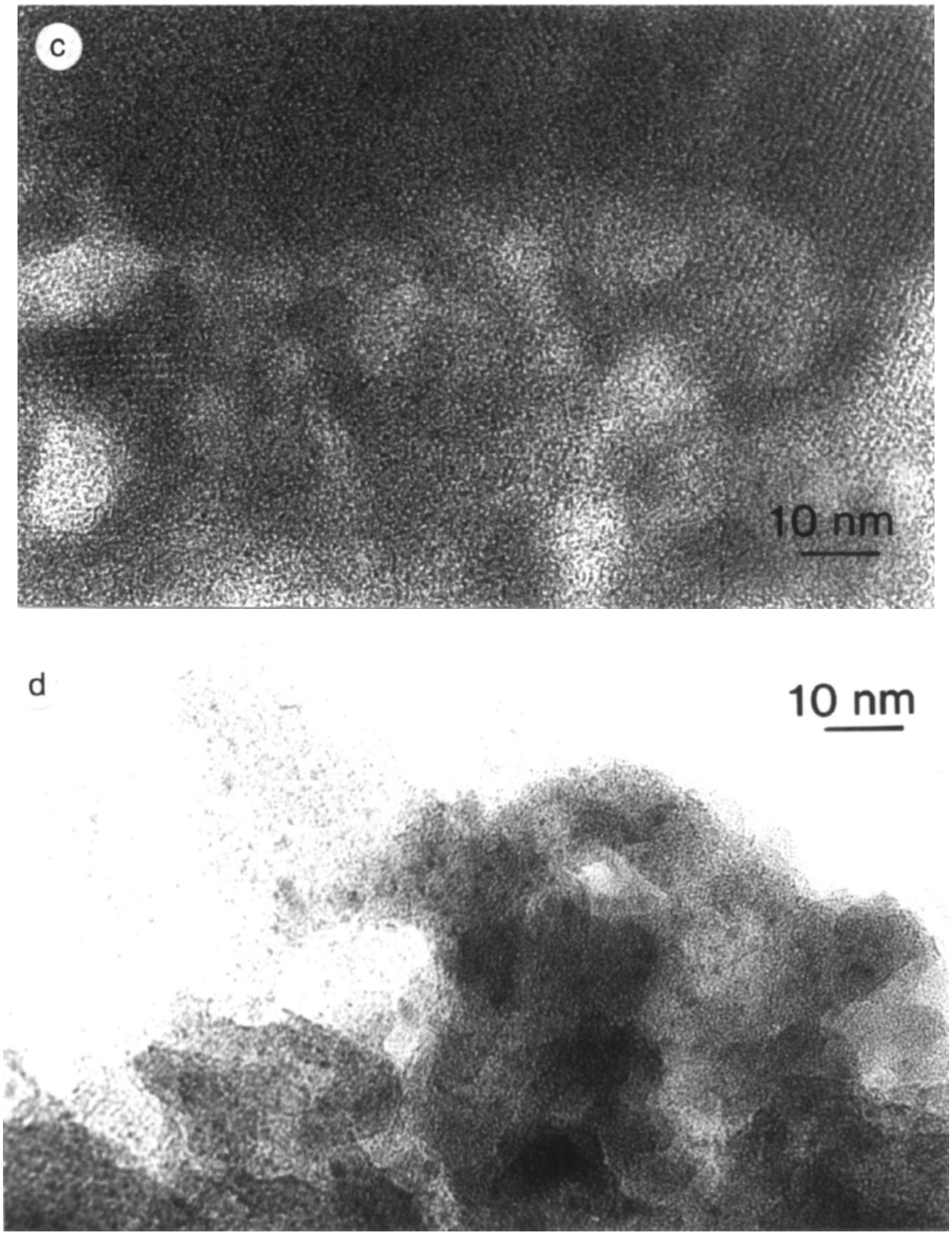

FIG. 2—*Continued*

(Fig. 2c) even smaller ones. It is assumed that the smallest particles are situated within the supercages, the size of which is 1.3 nm. The large particles formed after migration of the Ru phase, during sulfidation under H_2S/N_2, may be located on the outside of the zeolite particles or inside, which implies a partial destruction of the zeolite framework around the sulfide particles. Such an influence of the treatment conditions on the particle size is well documented for transition metal/zeolite catalysts. Welters *et al.* (5) have also shown the influence of the pretreatment conditions on the size and location of nickel sulfide in zeolite.

When large areas (of the size of the grain diameter) of the sulfided catalysts were analyzed by EDX, the sulfur to ruthenium ratios were almost similar to those obtained by chemical analysis; i.e., 4 for RuKYd (H_2S/N_2) and 2.4 for RuKYd (H_2S/H_2). When smaller zones were analyzed, the sulfur to ruthenium ratio decreased to 2.5 for RuKYd (H_2S/N_2) and circa 1.5 for RuKYd (H_2S/H_2). For this last sample, the sulfur to ruthenium ratio varied from one zone to another. While the ruthenium content appeared to be almost constant, the sulfur concentration changed. Moreover, when the electron beam was focused on the smallest

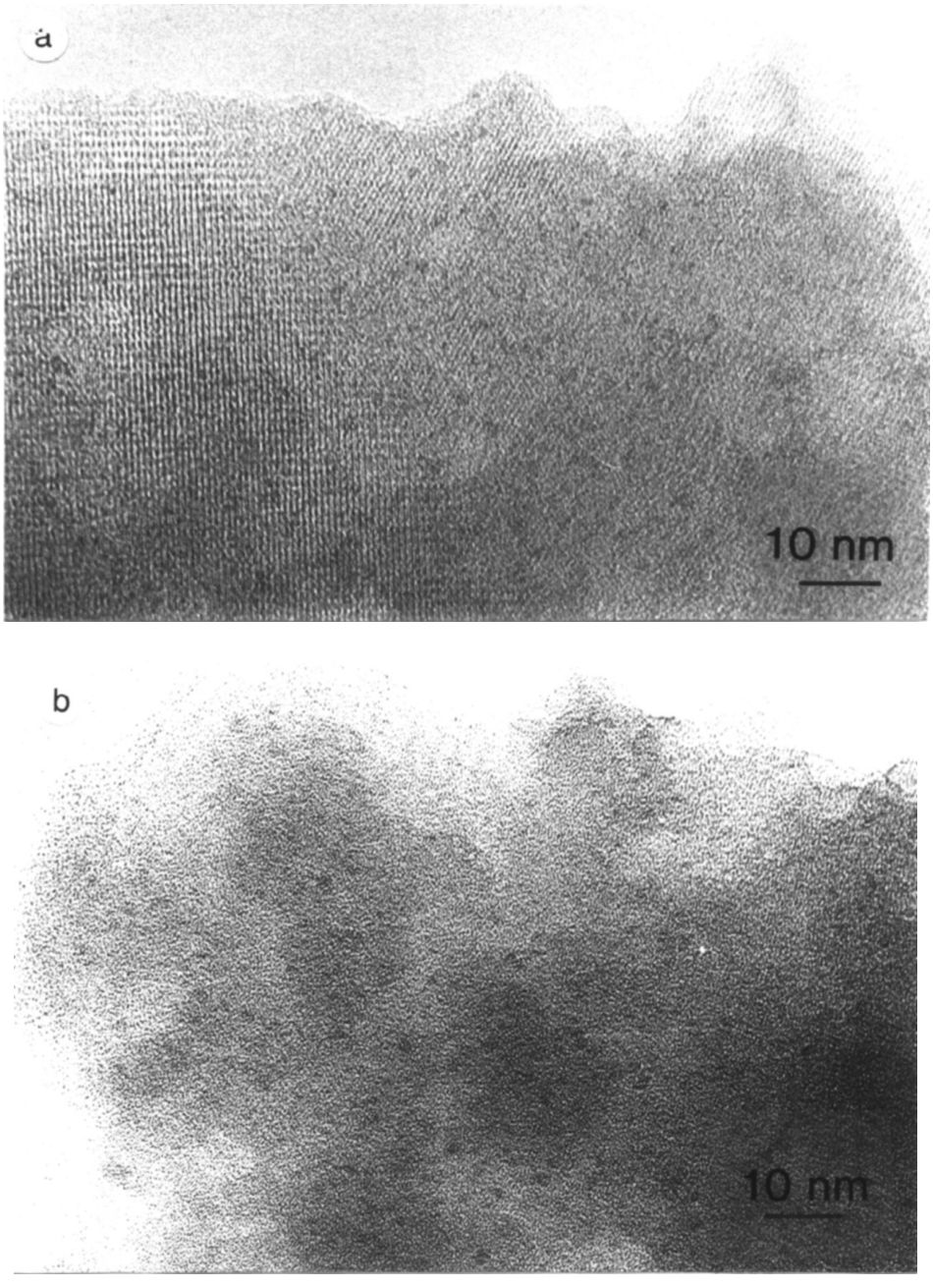

FIG. 3. Electron micrographs of RuKYd catalyst reduced by H_2 (a) before catalytic test and (b) after catalytic test.

particles, the amount of sulfur changed even during the examination. It appears that part of the sulfur was driven away by the electron beam when it was focused on very small areas. Consequently, for these small RuKYd particles, the EDX determination does not seem to be reliable enough. This is why TPR measurements were also performed to determine the sulfur concentrations.

After the catalytic test, RuKYd (H_2S/H_2) was not examined on thin cuts but on the whole grain in order to determine whether sintering and/or migration of RuS_2 particles had taken place outside or at the edge of the grain during the catalytic test. It can be seen in Fig. 2d that the particles are still dispersed homogeneously within the grains and that their diameter is about 1 nm.

In the reduced RuKYd (H_2), before (Fig. 3a) and after (Fig. 3b) the catalytic test, also examined on whole grains, Ru particles appear to be well dispersed, with particle sizes between 1 and 2 nm (even less for a few of them).

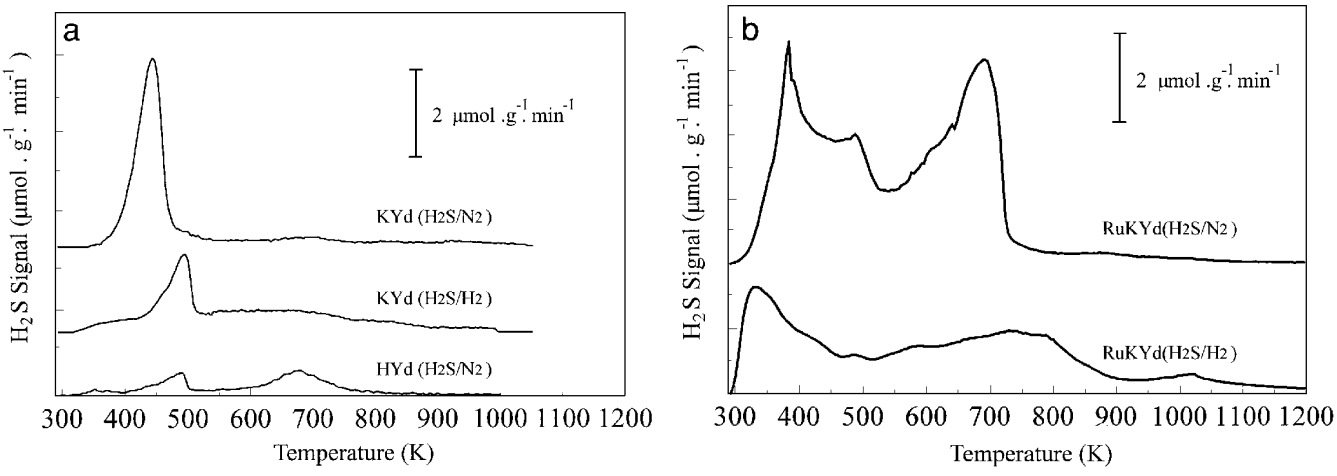

FIG. 4. Temperature-programmed reduction studies of (a) KYd and HYd sulfided by H_2S/N_2 or H_2S/H_2 and (b) RuKYd (H_2S/N_2) and RuKYd (H_2S/H_2), catalysts.

TPR

Supposing the EDX analysis to be erroneous, the sulfur on ruthenium ratios were much smaller for the particles than for the overall grains of zeolites, which may suggest that sulfur is associated with the zeolite. TPR of the KYd zeolite alone, sulfided by H_2S/H_2 or H_2S/N_2, are shown in Fig. 4a. A quite intense peak is observed at 430 K for the sulfidation by H_2S/N_2 and a smaller one at about 500 K for the sulfidation by H_2S/H_2. The amount of H_2S evolved from the HYd zeolite was small in comparison to the KYd zeolite, suggesting that the sulfur is associated mainly with the K^+ cations. A similar conclusion was drawn from the comparison of KY and HY nondealuminated zeolites (3). The TPR spectra of RuKYd (H_2S/H_2) and RuKYd (H_2S/N_2) are given in Fig. 4b. The difference between both types of sulfidation is clearly seen. In agreement with the EDX results, the amount of sulfur evolved from the catalyst sulfided by H_2S/H_2 is much smaller than that obtained after sulfidation by H_2S/N_2.

From the comparison of Figs. 4a and 4b it seems possible that, from the total amount of sulfur released during the TPR of RuKYd, a small part may be related to the K^+ cations of the zeolite support itself. Thus, the peak at 400 K present on KYd (H_2S/N_2) may be included in the low-temperature peak region of the TPR diagram of RuKYd (H_2S/N_2). However, it is not clear whether the peak at 500 K for KYd (H_2S/H_2) should be included in the TPR of RuKYd (H_2S/H_2), which presents two large bands below and above this temperature. In fact, the presence of ruthenium sulfide particles may induce a shift of the temperature of reduction of sulfur related to K^+ cation. Therefore, the S/Ru ratio cannot be determined accurately from TPR. Nevertheless, a bracket of values of these ratios could be calculated by deducting or not deducting the amount of H_2S evolved from the zeolite itself from the overall amount of H_2S observed for the catalyst (Table 2). Such calculations give 2.3 for RuKYd (H_2S/N_2) and 1.6 for RuKYd (H_2S/H_2) when the overall amount of sulfur is taken into account, and 1.9 and 1.2, respectively when it is not. Since the corresponding values obtained by EDX are 2.5 and 1.5, it is concluded that a reasonable agreement was obtained between both types of determination. It is also concluded that the sulfidation by H_2S/H_2 leads to a stoichiometry much lower than the value of 2 expected for RuS_2 particles, whereas this value was obtained for the sulfidation by H_2S/N_2.

EXAFS

Figure 5 allows the comparison of the Fourier transforms of Ru, RuS_2, and RuKYd (H_2S/H_2) before the test. This figure clearly demonstrates that for RuKYd (H_2S/H_2), after activation, the Ru atom is coordinated with S and Ru atoms. The evolution of the sample during the reaction can be followed in Fig. 6. The coordination in S decreases, whereas the coordination in Ru increases. Figure 7 gives an example of the quality of the modeling for RuKYd (H_2S/H_2) before the test.

Table 3 combines the results of EXAFS analysis of the various samples. This table does not include the values of

TABLE 2

Values of S/Ru Ratios Calculated by Deducting or Not Deducting the Amount of H_2S Evolved from the Zeolite Itself from the Overall H_2S Amount Observed for the Catalyst

Sample	Quantity of H_2S (μmol g^{-1})	Quantity of H_2S from zeolite (μmol g^{-1})	S/Ru total	S/Ru (taking into account the S from zeolite)
RuKYd (H_2S/H_2)	282	67	1.6	1.2
RuKYd (H_2S/N_2)	414	77	2.3	1.9

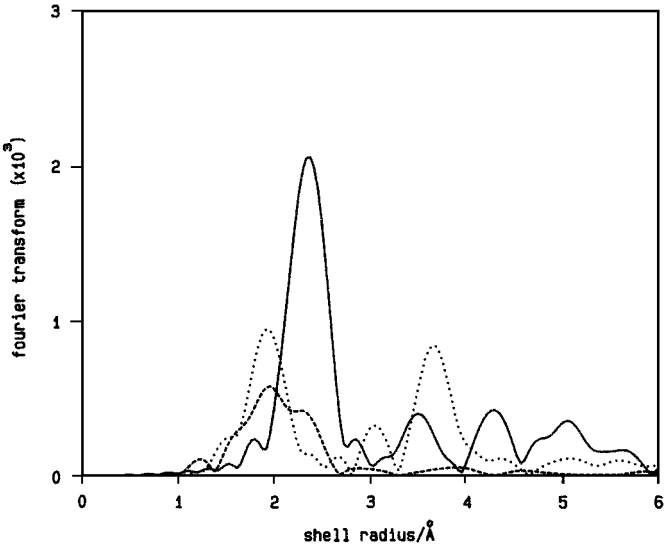

FIG. 5. Comparison of the Fourier transforms of metal Ru (solid line), RuS_2 (dotted line), and RuKYd (H_2S/H_2) (dashed line) before testing sample.

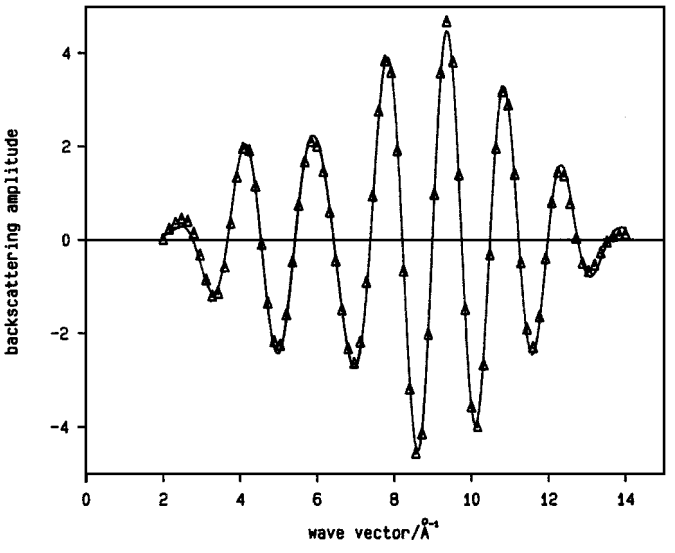

FIG. 7. Modeling of the first coordination sphere of RuKYd (H_2S/H_2) before the test; solid line, computed curve; triangles, experimental curve.

the energy adjustable parameter, ΔE. After the optimization process it always remains in the range ± 2 eV around the value used as references for the pure compounds bulk Ru and RuS_2, whatever the bond type and the sample.

The calculated lengths of Ru–Ru and Ru–S bonds are slightly lower than in the bulk reference compounds. In the case of the Ru–Ru bond, this difference is larger than the currently admitted value (0.2 Å) for the precision on the bond length obtained by EXAFS.

Absence of hydrogen in the sulfiding mixture avoids the formation of Ru–Ru bonds in the activated catalyst. Therefore, for RuKYd (H_2S/N_2), true ruthenium sulfide particles having the RuS_2 structure were formed. The Ru–S coordination number of 6.3 is in agreement with that of the reference RuS_2 sample.

In RuKYd (H_2S/H_2), the existence of Ru–S bonds was found, but there was also a relatively large number of Ru–Ru bonds corresponding to ruthenium metal. Sulfidation by $DMDS/H_2$ gives a catalyst containing an even greater number of Ru–Ru bonds. These results suggest that the active phase is composed of ruthenium sulfide and small domains of ruthenium metal. It can be seen in Table 3 that, after the catalytic test, all catalysts RuKYd (H_2S/N_2), RuKYd (H_2S/H_2), and RuKYd ($DMDS/H_2$) were found to be in similar states. Thus, after tetralin conversion we always observe the formation of Ru–Ru bonds together

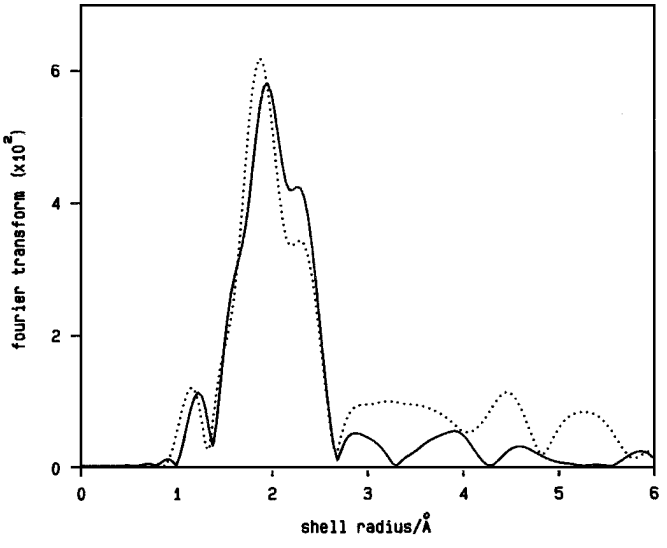

FIG. 6. Comparison of the Fourier transforms of RuKYd (H_2S/H_2) after (solid line) and before (dotted line) the test.

TABLE 3

Results of EXAFS Analysis

Sample	Ru–S			Ru–Ru			Q
	n	R(Å)	$\Delta\sigma^2$(Å^2)	n	R(Å)	$\Delta\sigma^2$(Å^2)	(%)
Ruthenium	—	—	—	12	2.677	—	—
RuS_2	6	2.354	—	—	—	—	—
RuKYd (H_2S/N_2) before test	6.3	2.33	0.0033	—	—	—	13.4
RuKYd (H_2S/N_2) after test	4.9	2.33	0.0027	4.7	2.63	0.0082	8.1
RuKYd (H_2S/H_2) before test	5.1	2.33	0.0036	3.5	2.62	0.0019	8.3
RuKYd (H_2S/H_2) after test	4.7	2.33	0.0020	5.1	2.63	0.0039	4.8
RuKYd ($DMDS/H_2$) before test	4.6	2.32	0.0023	5.4	2.64	0.0049	5.7
RuKYd ($DMDS/H_2$) after test	4.7	2.34	0.0025	5.5	2.63	0.0038	2.6

with an increase in the total mean coordination number around ruthenium. When the catalyst already exhibits Ru–Ru bonds before the reaction we observe a slight increase in the mean coordination number of ruthenium, indicating a growth of the ruthenium metal domains.

Tetralin Hydrogenation

First, the zeolite KYd and the catalyst RuKYd were sulfided by using the standard sulfiding procedure (15% H_2S/H_2, 673 K, 0.1 MPa), and their activities for the hydrogenation of tetralin were compared. The activity of the zeolite alone was negligible (0.08×10^{-7} mol/g s) in comparison to that of the RuKYd catalyst (from 2.4 to 9.4×10^{-7} mol/g s). The $NiMo/Al_2O_3$ industrial catalyst also showed a much lower activity (0.25×10^{-7} mol/g s).

The sulfidation of the catalyst using a H_2S/H_2 mixture gave the highest activity (9.4×10^{-7} mol/g s). The difference between the results obtained with H_2S/H_2 and H_2S/N_2 (2.4×10^{-7} mol/g s) was expected since as shown above the dispersion is different depending on whether the catalyst is sulfided in the presence or absence of hydrogen. However, this was not the case for the sulfidation by $DMDS/H_2$ (4×10^{-7} mol/g s), which leads to very small particles as obtained for H_2S/H_2. In addition to the problem of dispersion, two other parameters could be important, i.e., the stoichiometry and the possible presence of coke. Since the EXAFS results show that the nature of the active phases after the test are very similar whatever the initial procedure, this could not explain the difference in reactivity observed for the catalysts sulfided by $DMDS/H_2$ and H_2S/H_2. Therefore, the detrimental effect of the sulfidation by DMDS might be ascribed to coke formation on the acidic sites of the zeolite. In fact, temperature-programmed oxidation studies show a CO_2 release peak at 633 K, whereas no peak was observed for RuKYd (H_2S/H_2). The presence of coke obviously impedes the catalytic properties of the sample sulfided by DMDS as documented in Ref. (14).

In order to examine the influence of the H_2S partial pressure during the catalytic reaction, two different sets of reactions were carried out with RuKYd (H_2S/H_2). In the first one, the catalyst was allowed to deactivate for 80 h under the normal H_2S concentration in H_2 (1.875%) (Fig. 8). In the second one, the H_2S partial pressure was varied. When the H_2S pressure decreased, the rate increased until a maximum was reached for the partial pressure of 1000 ppm. At this pressure, the deactivation was very fast, which suggests that the nature of the catalyst is changing. For H_2S concentrations lower than 1000 ppm, the rate decreased with the H_2S concentration. At the end of the experiment the initial H_2S partial pressure was restored (1.875% H_2S/H_2), and the hydrogenation rate reached a value a little lower than that observed for the catalyst when it deactivates for the same period of time under the initial mixture of reactants. This indicates that, although lowering the concentration of

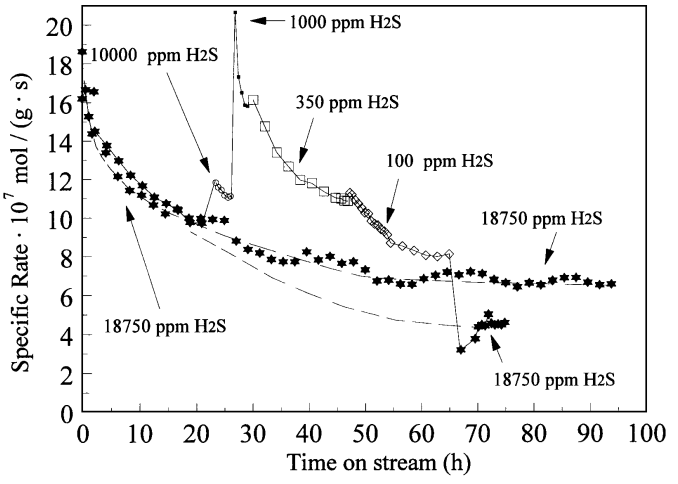

FIG. 8. The influence of the H_2S partial pressure during the catalytic test on the hydrogenation activity of the sulfided RuKYd (H_2S/H_2) catalyst. The sulfidation was performed with 15% H_2S/H_2 at $T = 673$ K and $P = 0.1$ MPa.

H_2S in the reactor leads initially to higher catalyst activities, there is an optimum H_2S concentration below which the catalyst activity starts to diminish, due probably to an irreversible modification of the surface. Since EXAFS experiments have shown that the particles contain both RuS_2 and Ru metal-like domains, it is assumed that lowering the H_2S concentration leads to the formation of larger crystallites of Ru metal which may be less active than the sulfide phase in the presence of high amounts of H_2S. To examine this hypothesis further, two other sets of experiments were performed.

RuKYd (H_2S/H_2) was allowed to deactivate for 18 h (Fig. 9) under the normal H_2S concentration in H_2

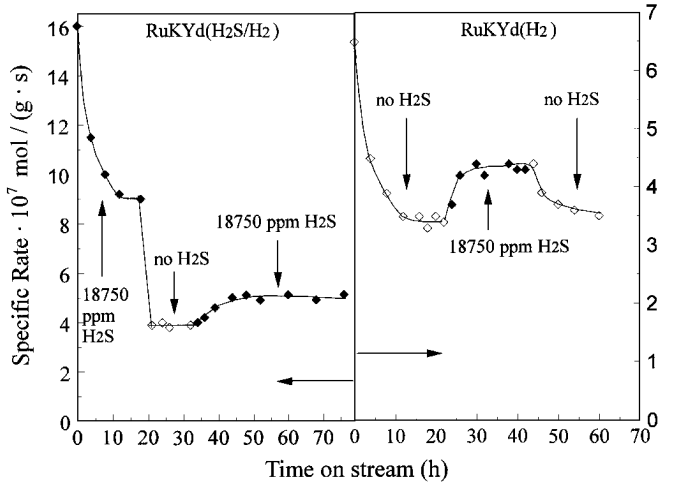

FIG. 9. The influence of the complete removal of H_2S from the catalytic test on the hydrogenation activities of sulfided RuKYd (H_2S/H_2) (left) and reduced RuKYd (H_2) (right) catalysts for tetralin hydrogenation. The sulfidation was performed with 15% H_2S/H_2 at $T = 673$ K and $P = 0.1$ MPa.

(1.875%); then H_2S was completely removed from the reactor feed. Upon removal of H_2S the hydrogenation rate dropped by about 60%. After 15 h on stream time, the initial H_2S concentration was restored, which led to an enhancement of the activity, but the level of activity was clearly smaller than expected without modifying the H_2S concentration. In another experiment, the catalyst was not sulfided but only reduced by hydrogen. The catalytic test was carried out in the same setup as for all the experiments but without addition of H_2S. After 20 h, 1.875% of H_2S was introduced, which led to an activity enhancement. The removal of H_2S restored the first level of activity. It is particularly interesting to note that the rates obtained in the presence or absence of H_2S are coherent for the three sets of experiments. From these results it is concluded that the dispersion of the ruthenium metal phase, formed either by direct reduction or during a few hours of catalytic testing without H_2S, is probably similar. This ruthenium metal phase is less active than the sulfided phase.

DISCUSSION

Nature of the Ruthenium Phase

The pyrite structure of RuS_2 can be represented as a modified NaCl structure with two interpenetrating fcc sublattices. Ru atoms are located on one fcc sublattice and $(S–S)^{2-}$ groups are placed on the other (15). In the cubic unit cell each ruthenium atom is surrounded by six S–S pairs arranged in a slightly distorted octahedron. Each sulfur atom is bonded to three metal ions and to another sulfur atom. There is only one type of S–S and Ru–S bond in this structure. For a single unit cell structure, there are 14 metal atoms, all of them being at the surface, and 13 sulfur pairs associated with the Ru atoms, 12 of them located at the surface. A crystallographic model based on a three-dimensional growth of the cubic unit cell allows the calculation of the amount of Ru and S–S ions present either at the surface of the crystallite or in the entire particle as a function of the particle size (16). From this cubic model it is possible to derive a truncated octahedron structure which provides a spherical morphology similar to the HREM observations. The smallest particle is composed of 38 Ru atoms (32 on the surface) and 122 sulfur atoms corresponding to a complete sulfur coordination of Ru of 6 (Fig. 10a). The sulfur to ruthenium ratio is then equal to 3.21 and the particle size to 1.1 nm. The removal of superficial sulfur atoms would lead to a mean coordination number n(Ru–S) of 3.9 and a sulfur on ruthenium ratio of 1.1.

Since it was shown that the geometrical models appear to be correct for the interpretation of the TPR patterns (16, 17), they might be utilized for the modeling of the results obtained here by the different techniques. However, this could be done only for samples uniformly dispersed such as RuKYd (H_2S/H_2) and RuKYd (DMDS/H_2), but not for RuKYd (H_2S/N_2), which presents particle sizes ranging from 3 to 5 nm and below. For the first sample, the particle size is circa 1 nm, which corresponds to the smallest particle size of the above model. The EXAFS measurements indicate the presence of Ru–S and Ru–Ru metal bonds, whose presence should be taken into account. If one hexagonal face (111 plane) of the truncated octahedron is naked from its sulfur upper atoms, then the mean coordination number n(Ru–S) is reduced to 5. Following

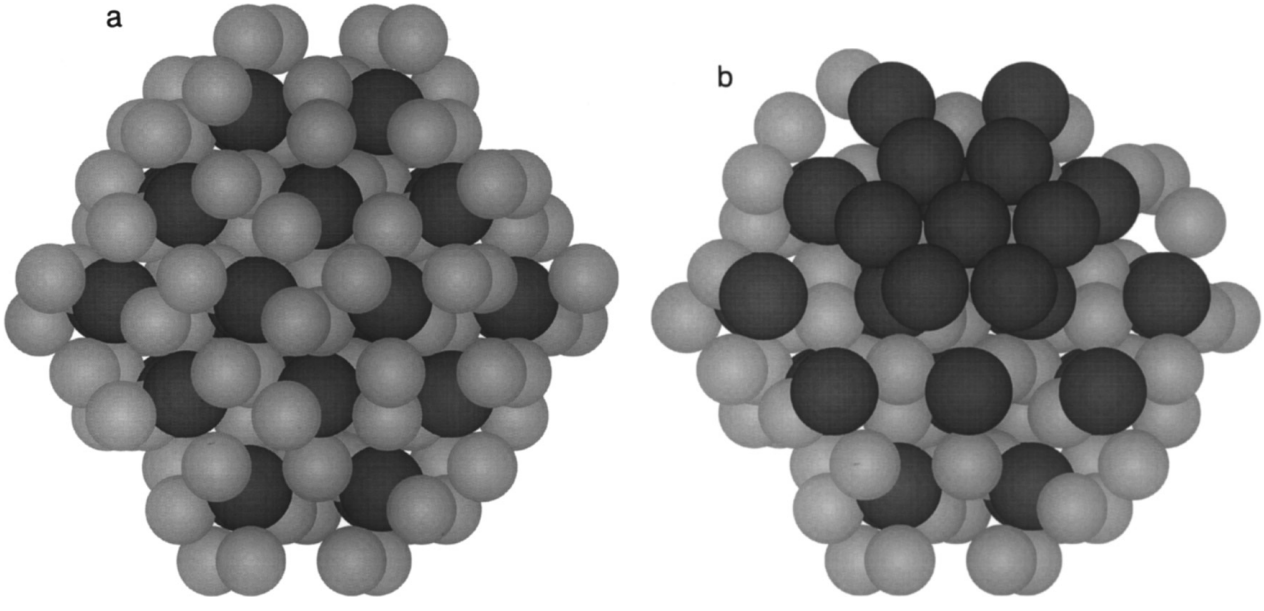

FIG. 10. Truncated octahedron of a particle of (a) fully sulfided and (b) partially reduced ruthenium disulfide.

the partial desulfurization of the particle described above, the remaining hexagon of Ru atoms aggregates breaking most of the Ru–S bonds located below and creates metal–metal bonds (Fig. 10b). The corresponding Ru–Ru coordination number is equal to 3.4. This model is consistent with the EXAFS results obtained for RuKYd (H_2S/H_2), that is, 5.1 for the mean Ru–S coordination number and 3.5 for the Ru–Ru coordination number. The resulting sulfur to ruthenium ratio of the overall particles corresponds roughly to 2. However, the experimental value determined by several techniques is lower, i.e., 1.7. To account for this experimental value, it is proposed to add to the phenomenon of metal clusterization on one face of the particle a random elimination of sulfur atoms on the other faces of the particles. This sulfur elimination would not destroy the RuS_2 structure. In fact, it was shown for unsupported RuS_2 (18) that the range of stability of the pyrite phase is very broad. For this catalyst, a complete depletion of the surface of the particles in sulfur is obtained without any noticeable modification of the structural and morphological properties. Such a random elimination of sulfur from the surface of the ruthenium sulfide particles dispersed in the KYd zeolite leads to a slight decrease in the n(Ru–S) coordination number.

After the test, the Ru–Ru coordination number increases to 5.1, which is better represented by a three-dimensional particle of about 13 Ru atoms located either on the RuS_{2-x} particle or separated. This indicates that the metallic particle growth is detrimental to the RuS_2 cluster which leads to a small decrease in the Ru–S coordination number from 5.1 to 4.7. Due to the very small sizes of the particles, it is not possible to determine whether the Ru metal phase is totally separated from the RuS_{2-x} phase or whether it is in close contact. The catalytic activity measurements, which indicate a partial reversibility of the desulfurization state of the catalyst, favor the second hypothesis. The results obtained for RuKYd ($DMDS/H_2$) are very similar, but no evolution of the catalyst is observed before and after the test, this sample being, before the test, less sulfurized than when H_2S/H_2 is used as the sulfiding mixture.

The representation of the ruthenium phase dispersed in the KYd zeolite which emerges from the EXAFS, HREM, EDX, and TPR results is therefore a cluster of less than 50 ruthenium atoms composed of a ruthenium sulfide phase and a metallic phase in close interaction, the proportion of each phase depending on the experimental conditions.

In this model, the metal domain is located on a face of the sulfide particle but other hypotheses could be envisaged, either a metallic core covered by a sulfide phase or distinct particles. The present model appears the most satisfying to take into account the very low Ru–Ru coordination number of the metal-like phase observed for RuKYd (H_2S/H_2) before catalytic testing, which suggests that this cluster is only two dimensional.

Relevance to Catalytic Properties

The nature of catalyst after the test is similar whatever the activation conditions, as shown by EXAFS, the only difference being the dispersion (rather poor for RuKYd (H_2S/N_2) and the formation of coke for RuKYd ($DMDS/H_2$), which explains the difference in activity. Consequently, the following discussion is related only to RuKYd (H_2S/H_2).

The high activity for hydrogenation reactions of unsupported RuS_2 in comparison to the other transition metal sulfides is well documented (1). Furthermore, the study of the reduction process of this catalyst has shown that as long as the stability of the catalyst is preserved (until about 50% of sulfur removal), an increase in the degree of desulfurization brings about a very large increase in activity for butene hydrogenation and H_2–D_2 exchange reactions. It was then concluded that the active sites for these reactions are coordinatively unsaturated ruthenium atoms present on the surface of the ruthenium sulfide phase (18). The pure bulky ruthenium metal phase appears much less active, which was attributed to poisoning by residual sulfur. These conclusions concerning the unsupported ruthenium sulfide can account for the high activity of the present catalyst which is composed of very small particles of ruthenium sulfide containing mostly superficial ruthenium atoms which are not fully coordinated by sulfur. Nevertheless, it was also shown by EXAFS that very small metal particles are present which may also be active. The dispersion of these particles is much higher than those formed by reduction of the unsupported ruthenium sulfide phase which may change their resistance to poisoning. The present results are not very different for RuKYd (H_2) and RuKYd (H_2S/H_2) although slightly smaller for the metallic catalyst. The discrimination between a poisoned metal and a sulfide, proposed in the literature (19), is not relevant for this high dispersion state. In fact, reaction with sulfur rapidly induces a high sulfur coverage of the particle and then the thermodynamic feature resembles that of the sulfide and not that of the poisoned metal.

CONCLUSION

Zeolite Y-supported ruthenium sulfide catalysts, prepared by ion exchange and further sulfidation by H_2S/H_2, are very active for the hydrogenation of tetralin in the presence of H_2S. These properties are related to the nature of the active phase which consists of clusters of circa 50 ruthenium atoms of a ruthenium sulfide like phase located in the zeolite framework. In these clusters, almost all the ruthenium atoms are exposed which explains their very high activity. The purpose of using zeolite as supports of sulfide catalysts is then to stabilize highly dispersed particles. Apparently, an equilibrium state, between the metallic and the sulfide phase, is reached. Under these conditions, the nature of

the zeolite may have a significant effect on the electronic and catalytic properties of the particles. The role of the acid base properties of the zeolite is addressed in another study (20).

ACKNOWLEDGMENTS

This work was carried out within the framework of the program "Hydrogenation of Aromatics" supported by ELF, IFP, TOTAL, and the CNRS-ECOTECH. We thank the European Community for a Human Capital and Mobility Program Fellowship granted to Vassilios KOUGIONAS. We are indebted to Dr. Frédéric FRECHARD and Mrs. Christiane LECLERCQ for their assistance in the catalyst modeling and electron microscopy studies.

REFERENCES

1. Lacroix, M., Boutarfa, N., Guillard, C., Vrinat, M., and Breysse, M., *J. Catal.* **120**, 473 (1989).
2. Harvey, T. G., and Matheson, T. W., *J. Catal.* **101**, 253 (1986).
3. Kougionas, V., Cattenot, M., Zotin, J. L., Portefaix, J. L., and Breysse, M., *Appl. Catal. A: General* **124**, 153 (1995).
4. Zotin, J. L., Cattenot, M., Portefaix, J. L., and Breysse, M., *Bull. Soc. Chim. Belg.* **104**, 213 (1995).
5. Welters, W. J. J., Vorbeck, G., Zandbergen, H. W., de Haan, J. W., De Beer, V. H. J., and Van Santen, R. A., *J. Catal.* **150**, 155 (1994).
6. Leglise, J., Manoli, J. M., Potvin, C., Djega-Mariadassou, G., and Cornet, D., *J. Catal.* **152**, 275 (1995).
7. Sugioka, M., *Science Technol.* **48**, 128 (1995).
8. Moraweck, B., and Renouprez, A. J., *Surf. Sci.* **106**, 35 (1981).
9. Lengeler, B., and Eisenberger, P., *Phys. Rev. B* **21**, 4507 (1980).
10. Nedler, J. A., and Mead, R., *Comp. J.* **7**, 308 (1965).
11. Yuan, S., Decamp, T., Lacroix, M., Mirodatos, C., and Breysse, M., *J. Catal.* **92**, 5184 (1988).
12. Borgna, A., Moraweck, B., and Renouprez, A. J., *J. Chim. Phys. Biol.* **86**, 1719 (1989).
13. Schwartz, L. H., and Cohen, J. B., *in* "Diffraction from Materials," p. 295. Academic Press, New York, 1977.
14. Mhaouer, M., Lemberton, J. L., and Pérot, G., *Catal. Today* **29**, 241 (1996).
15. Sutarno, O., Knop, O., and Reid, I. G., *Can. J. Chem.* **45**, 1391 (1967).
16. Geantet, C., Calais, C., and Lacroix, M., *C.R. Acad. Sci. Paris* **315**, 439 (1992).
17. De Los Reyes, J. A., Vrinat, M., Geantet, C., and Breysse, M., *Catal. Today* **10**, 645 (1991).
18. Lacroix, M., Mirodatos, C., Breysse, M., Decamp, T., and Yuan, S., *in* "New Frontiers in Catalysis" (L. Guczi, F. Solymosi, and P. Tétényi, Eds.), Vol. A, p. 597. Akadémiai Kiado, Budapest, 1993.
19. Wise, H., McCarty, J., and Oudar, J., *in* "Deactivation and Poisoning of Catalysts" (J. Oudar and H. Wise, Eds.), Chemical Industries, Vol. 20, p. 45. Dekker, New York, 1985.
20. Breysse, M., Cattenot, M., Kougionas, V., Lavalley, J. C., Mauge, F., Portefaix, J. L., and Zotin, J. L., in preparation.